JACS
JOURNAL OF THE AMERICAN CHEMICAL SOCIETY
Article
pubs.acs.org/JACS

Fluorescent Base Analogue Reveals T-Hg^{II}-T Base Pairs Have High Kinetic Stabilities That Perturb DNA Metabolism

Olivia P. Schmidt, Guillaume Mata, and Nathan W. Luedtke*

Department of Chemistry, University of Zürich, Winterthurerstrasse 190, CH-8057 Zürich, Switzerland

Supporting Information

ABSTRACT: The thymidine analogue ^{DMA}**T** was used for the first fluorescence-based study of direct, site-specific metal binding reactions involving unmodified nucleobases in duplex DNA. The fluorescence properties of ^{DMA}**T**-A base pairs were highly sensitive to mercury binding reactions at T-T mismatches located at an adjacent site or one base pair away. This allowed for precise determination of the local kinetic and thermodynamic parameters of T-Hg^{II}-T binding reactions. The on- and off-rates of Hg^{II} were surprisingly slow, with association rate constants (k_{on}) $\approx 10^4-10^5$ M^{-1} s^{-1}, and dissociation rate constants (k_{off}) $\approx 10^{-4}-10^{-3}$ s^{-1}; giving equilibrium dissociation constants (K_d) = 8−50 nM. In contrast, duplexes lacking a T-T mismatch exhibited local, nonspecific Hg^{II} binding affinities in the range of K_d = 0.2−2.0 μM, depending on the buffer conditions. The exceptionally high kinetic stabilities of T-Hg^{II}-T metallo-base pairs (half-lives = 0.3−1.3 h) perturbed dynamic processes including DNA strand displacement and primer extension by DNA polymerases that resulted in premature chain termination of DNA synthesis. In addition to providing the first detailed kinetic and thermodynamic parameters of site-specific T-Hg^{II}-T binding reactions in duplex DNA, these results demonstrate that T-Hg^{II}-T base pairs have a high potential to disrupt DNA metabolism in vivo.

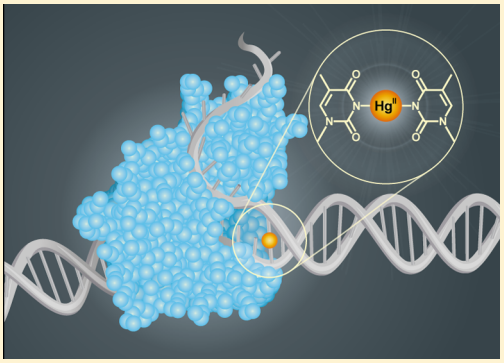

INTRODUCTION

Hg^{II} is infamous for being cytotoxic and mutagenic,[1] but the exact mechanisms for these activities are still unclear. In addition to oxidative stress,[2] Hg^{II} causes DNA point mutations,[3] DNA strand breaks,[4,5] and the inhibition of DNA synthesis and repair in live cells.[5,6] These activities could be the result of direct mercury−DNA binding interactions. When 5 μM $HgCl_2$ was applied to live cells for 4 h and the DNA harvested and analyzed, approximately 0.3% of base pairs contained mercury.[7] After 30 years of study, however, little is known about the composition or structure of these complexes. While many different metal-DNA binding modes are possible,[8] Hg^{II} preferentially binds to *N1* or *N7* of purines and to *N3* of thymidine residues in vitro.[9] In 2006, Ono and co-workers reported that T-T mismatches in duplex DNA exhibited stoichiometric binding of Hg^{II} ions in vitro, giving duplexes with approximately the same thermal stabilities as duplexes containing T-A base pairs.[10] The preferred Hg^{II} binding site was found to be the *N3* positions of two deprotonated thymine residues (Figure 1a).[11] A crystal structure of duplex DNA containing two such T-Hg^{II}-T base pairs revealed minimal distortion of the B-form duplex.[12] In addition to structural similarities, T-Hg^{II}-T can serve as a functional mimic of T-A base pairs by stabilizing T-T during DNA primer extension,[13] and by causing the enzymatic misincorporation of dTTP across from thymidine to give T-Hg^{II}-T base pairs.[14] These activities provide a potential mechanism for the formation of T-Hg^{II}-T base pairs in S-phase cells.

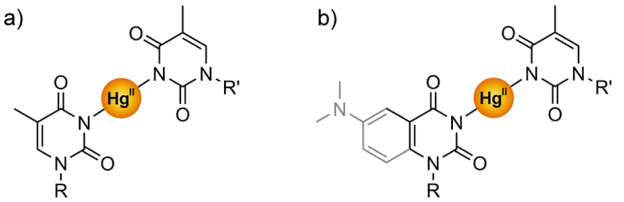

Figure 1. (a) T-Hg^{II}-T base pair and (b) ^{DMA}**T**-Hg^{II}-T base pair (R, R′ = duplex DNA).

Given the potentially broad importance of T-Hg^{II}-T base pairs in both biological and material sciences,[15] a wide variety of spectroscopic methods have been used to characterize their properties including UV,[10,16] Raman,[17] CD,[18] NMR,[19] EPR,[19c] ITC,[20] and fluorescence.[21] With the exception of high resolution structural analyses, these methods revealed changes in global properties resulting from both specific and nonspecific binding interactions. To our knowledge, there are no previous studies that reported the exact kinetic and thermodynamic parameters of local, site-specific T-Hg^{II}-T binding reactions in duplex DNA. These values are important for understanding the potential biological impact and material properties of T-Hg^{II}-T base pairs.

Fluorescent nucleobase analogs (FBAs) can facilitate highly sensitive biophysical measurements with single-base resolu-

Received: August 29, 2016
Published: October 6, 2016

DOI: 10.1021/jacs.6b09044
J. Am. Chem. Soc. 2016, 138, 14733−14739

tion.[22,23] FBAs are therefore ideal candidates for characterizing local binding interactions,[24] but only a few previous studies have utilized FBAs as probes of transition metal binding.[25] In these cases, the FBA directly participated in the binding reaction and therefore provided little or no information about native DNA-metal interactions. In other examples,[24] ligand binding caused conformational changes that impacted the FBA's microenvironment and therefore fluorescence properties in an indirect way. There are no previous examples of native, site-specific metal-nucleobase binding interactions being directly reported by an FBA. This would provide a powerful tool for determining the kinetic and thermodynamic parameters of local metal binding reactions. With this goal, we recently synthesized a new fluorescent thymidine mimic "^{DMA}**T**" that exhibits the same base pairing preferences as native thymine residues.[26] Duplexes containing ^{DMA}**T**-A or ^{DMA}**T**-Hg^{II}-T base pairs (Figure 1b) exhibited the same global structures, thermal stabilities, and metal binding properties as wild-type duplexes containing T-A or T-Hg^{II}-T, respectively. Here we report the use of ^{DMA}**T**-T and ^{DMA}**T**-A for directly assessing the local kinetic and thermodynamic parameters of T-Hg^{II}-T binding reactions. Surprisingly, T-Hg^{II}-T complexes exhibited slow association and dissociation kinetics and perturbed dynamic processes including DNA strand displacement and enzymatic synthesis. T-Hg^{II}-T complexes therefore have a high potential to disrupt DNA metabolism in vivo.

RESULTS

Thermodynamic Analysis of T-Hg^{II}-T Binding. To the best of our knowledge, isothermal titration calorimetry (ITC) was the only technique previously used to assess the thermodynamic parameters of Hg^{II} binding to T-T mismatches in duplex DNA.[20] In this approach, Hg^{II} was titrated into concentrated solutions of DNA (40 μM) and the changes in heat flow were measured. The results suggested a modest equilibrium dissociation constant (K_d) = ~2 μM for DNA sequences containing a single T-T mismatch.[20] Given the exceptionally high sensitivity of fluorescence measurements, we were able to use dilute solutions of DNA (25 nM, Figure 2) for equilibrium titrations (Figure 3). Initial binding experiments were conducted in the same noncoordinating buffer previously

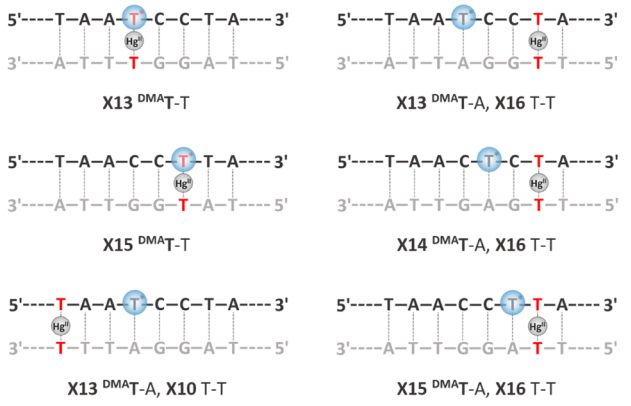

Figure 2. Variable regions (underlined) and names of DNA sequences used in these studies: **X13**, 5′-CCC-TAA-CCC-TAA-XCC-TAA-CCC-3′; **X14**, 5′-CCC-TAA-CCC-TAA-CXC-TAA-CCC-3′; **X15**, 5′-CCC-TAA-CCC-TAA-CCX-TAA-CCC-3′; where **X** = T or T* (^{DMA}**T**). See Tables S1 and S2 (SI) for a complete list of all reported duplexes.

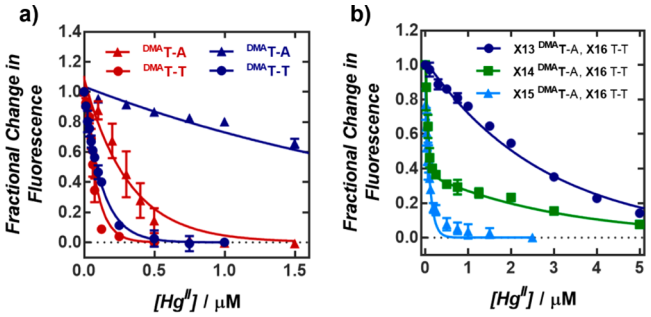

Figure 3. (a) Normalized changes in fluorescence of "**X13** ^{DMA}**T**-A" (triangles) or "**X13** ^{DMA}**T**-T" (circles) upon addition of Hg^{II} in a noncoordinating buffer (red) or metal-coordinating buffer (blue). (b) Fluorescence quenching of three different duplexes containing a T-T mismatch fixed at position **X16** and a ^{DMA}**T**-A base pair at position **X13**, **X14**, or **X15**. All DNA samples (25 nM) were incubated with variable concentrations of $Hg(ClO_4)_2$ at 25 °C for 1 h prior to reading (λ_{ex} = 370 nm, λ_{em} = 500 nm). Samples in (a) contained either 10 mM cacodylic acid, 100 mM $NaClO_4$ (pH = 6.8) or 200 mM Na_2HPO_4, 100 mM citric acid, 100 mM $NaNO_3$ (pH = 7.35). Samples in (b) were prepared in the phosphate-citrate buffer. See Figures S2–S4 for raw data.

reported for ITC-based measurements (10 mM cacodylic acid, 100 mM $NaClO_4$ (pH = 6.8)).[20] Hg^{II} was titrated into solutions of 21-mer duplex DNA containing either a ^{DMA}**T**-T mismatch (red circles, Figure 3a), or a ^{DMA}**T**-A base pair at position **X13** (red triangles, Figure 3a). After equilibrating the DNA with variable Hg^{II} concentrations for 1 h at 25 °C, the fluorescence intensities of each sample were measured. By fitting the data to a monophasic equation, K_d values were determined (eqs 1–4, SI). To our surprise, both duplexes exhibited very high Hg^{II} affinities under these conditions, with a K_d = 43 ± 6 nM for the duplex containing the ^{DMA}**T**-T mismatch and a K_d = 210 ± 40 nM for the DNA containing a ^{DMA}**T**-A base pair with no T-T mismatch. We reasoned that this small, 5-fold difference between mismatch-specific and non-specific DNA binding affinities would complicate the study of association kinetics under these conditions. To increase the specificity of binding (blue symbols, Figure 3a), the stringency of the reaction was increased by using a phosphate-citrate buffer (200 mM Na_2HPO_4, 100 mM citric acid and 100 mM $NaNO_3$ (pH = 7.35)) that reversibly coordinates to mercury ions.[27] Remarkably, a very similar affinity was measured for the DNA containing a ^{DMA}**T**-T mismatch in both coordinating (K_d = 77 ± 4 nM) and noncoordinating buffers (K_d = 43 ± 6 nM). In contrast, DNA containing ^{DMA}**T**-A and no T-T mismatch exhibited a 10-fold lower affinity (K_d = 1.97 ± 0.08 μM) in the coordinating versus noncoordinating buffer. Given the large improvement in binding specificity, we selected the phosphate-citrate buffer for subsequent experiments.

To evaluate the ability of a ^{DMA}**T**-A base pair to report the formation of a wild-type T-Hg^{II}-T complex at a neighboring or proximal site, duplexes were prepared containing a T-T mismatch at position **X16** and a ^{DMA}**T**-A base pair at position **X13**, **X14**, or **X15** (Figure 2). The duplex "**X13** ^{DMA}**T**-A, **X16** T-T" containing two intervening base pairs between ^{DMA}**T**-A and T-T exhibited the same concentration-dependent fluorescence response (apparent K_d = 1.96 ± 0.05 μM, Figure 3b) as did duplex "**X13** ^{DMA}**T**-A" containing no T-T mismatch (K_d = 1.97 ± 0.08 μM, Table 1). This indicated that in the case of "**X13** ^{DMA}**T**-A, **X16** T-T" the probe was positioned too far away

DOI: 10.1021/jacs.6b09044
J. Am. Chem. Soc. 2016, 138, 14733–14739

Table 1. Equilibrium Dissociation Constants (K_d) of Hg^{II} Binding to ^{DMA}T-Containing Duplex DNAs[a]

sequence	K_d (nM), nonspecific	K_d (nM), T-T-specific
X13 ^{DMA}**T**-A	1970 ± 80	n.o.[b]
X13 ^{DMA}**T**-T	n.o.[b]	77 ± 4
X13 ^{DMA}**T**-A, **X16** T-T	1960 ± 50	n.o.[b]
X14 ^{DMA}**T**-A, **X16** T-T	2200 ± 90	34 ± 12
X15 ^{DMA}**T**-A, **X16** T-T	n.o.[b]	57 ± 7

[a]Reported values = mean ± standard deviation from three independent measurements. Samples contained 25 nM DNA in an aqueous buffer containing 200 mM Na_2HPO_4, 100 mM citric acid, and 100 mM $NaNO_3$ (pH = 7.35). K_d values were calculated by fitting quenching data to a monoexponential curve (eqs 1–4, SI), except for "**X14** ^{DMA}**T**-A, **X16** T-T" which was fit to a biphasic curve (eq 5, SI). In all cases, R^2 values were ≥0.94. For duplex DNA sequences, see Table S1, SI. [b]n.o. = not observed.

(~10 Å) from T-T to report site-specific T-Hg^{II}-T association. This is consistent with heavy-atom fluorescence quenching effects that act over very short distances. In contrast, the duplex "**X15** ^{DMA}**T**-A, **X16** T-T" with no intervening base pair between ^{DMA}**T**-A and T-T exhibited the same apparent affinity (K_d = 57 ± 7 nM) as observed for duplex "**X13** ^{DMA}**T**-T" (K_d = 77 ± 4 nM, Table 1). These results suggest that the ^{DMA}**T**-A base pair can report Hg^{II} binding of a neighboring T-T mismatch with little or no impact on the affinity of the reaction. Kinetics analyses (Table 2) further support this conclusion. Interestingly, the duplex "**X14** ^{DMA}**T**-A, **X16** T-T" containing a single intervening base pair between ^{DMA}**T**-A and T-T exhibited a pronounced biphasic quenching curve (green squares, Figure 3b). The first component saturated at a 0.7 fractional decrease in fluorescence with an affinity consistent with specific T-Hg^{II}-T binding (K_d = 34 ± 12 nM), while the second component exhibited an apparent affinity indicative of nonspecific binding (apparent K_d = 2.20 ± 0.09 μM, Table 1, overall goodness of fit (R^2) = 0.98). These results provided the first example of an experiment where both the specific and nonspecific Hg^{II} binding affinities could be derived from a single titration.

Kinetic Analysis of T-Hg^{II}-T Binding. Time-dependent changes in fluorescence were used to measure Hg^{II} association rates by duplexes containing a single ^{DMA}**T**-T mismatch at position **X13** or **X15**, or an unmodified T-T mismatch adjacent to a ^{DMA}**T**-A base pair in "**X15** ^{DMA}**T**-A, **X16** T-T". Control experiments with duplexes containing a ^{DMA}**T**-A base pair but no T-T mismatch exhibited an extremely rapid and small magnitude of fluorescence quenching (<10%) upon addition of Hg^{II} (Figures S6 and S7, SI). This nonspecific component was excluded from our data analysis. Association rates and rate constants (k_{on}) were determined using pseudo-first-order approximations (eqs 6–9, SI) at three mercury concentrations. Similar k_{on} values were obtained for all three duplexes, ranging from 0.8–9.0 × 10^4 s^{-1} (Table 2). These rate constants are about 10^5-fold lower than those reported for outer-sphere binding of divalent ions to polynucleotides.[28] This is consistent with the fact that T-Hg^{II}-T binding requires *N*3-H deprotonation to give a stable complex. It was unclear how this multistep process might impact our kinetics analyses, but the excellent agreement between the K_d values determined by both kinetic and thermodynamic methods indicate a negligible effect (Tables 1 and 2).

To measure the rate constants of mercury dissociation (k_{off}) from duplexes containing ^{DMA}**T**-Hg^{II}-T or T-Hg^{II}-T, a large excess of nonfluorescent duplex DNA containing a T-T mismatch was added as a passive Hg^{II} scavenger. The addition of 40 equiv of unlabeled DNA was needed to obtain a concentration-independent, first order dissociation curve (Figure 4b). By fitting the data to a single-order decay process,

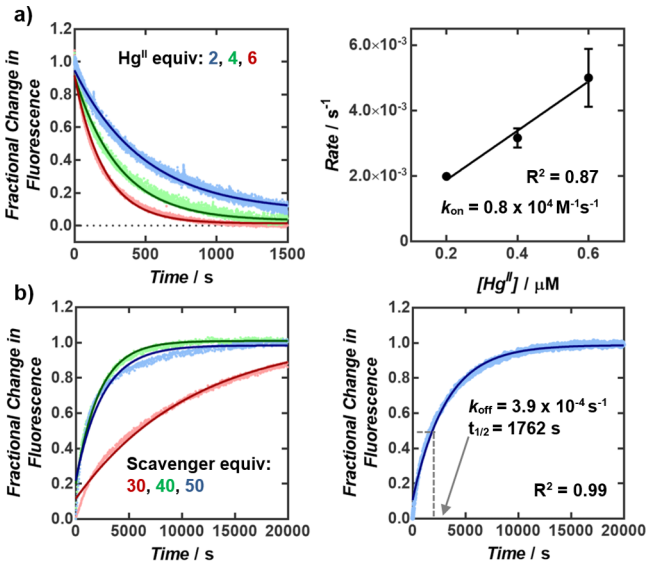

Figure 4. (a) Association of Hg^{II} to "**X13** ^{DMA}**T**-T" according to fluorescence changes (λ_{ex} = 370 nm, λ_{em} = 500 nm). Rate constants of association (k_{on}) were determined from the slopes of reaction rate versus Hg^{II} concentration. (b) Dissociation of Hg^{II} from "**X13** ^{DMA}**T**-T" upon the addition of unlabeled, T-T-containing duplex DNA of the same sequence. ^{DMA}**T**-Hg^{II}-T and T-Hg^{II}-T base pairs were formed by preincubation of the DNA with 2 equiv of $Hg(ClO_4)_2$ for 3 h. All samples contained 0.1 μM (k_{on}) or 4 μM (k_{off}) of DNA in aqueous buffer (200 mM Na_2HPO_4, 100 mM citric acid, and 100 mM $NaNO_3$ (pH = 7.35)). For raw data, see Figures S8–S10, SI.

Table 2. Rate Constants of Association (k_{on}), Dissociation (k_{off}), and Calculated Equilibrium Dissociation Constants (K_d) of Hg^{II} Binding to ^{DMA}T-T or T-T in Duplex DNA[a]

sequence	k_{on} (M^{-1} s^{-1})	k_{off} (s^{-1})	K_d (nM)[c]
X13 ^{DMA}**T**-T	0.8 ± 0.2 × 10^4	4.0 ± 0.5 × 10^{-4}	50 ± 14
X15 ^{DMA}**T**-T[b]	1.9 ± 0.1 × 10^4	1.5 ± 0.2 × 10^{-4}	8.0 ± 1.1
X15 ^{DMA}**T**-A, **X16** T-T	9.0 ± 2.0 × 10^4	9.0 ± 4.0 × 10^{-4}	10 ± 5.0

[a]Reported values = mean ± standard deviation from three independent measurements. Dissociation rate constants were determined by addition of 50 equiv of unlabeled DNA containing a T-T mismatch. All samples were prepared in aqueous buffer (200 mM Na_2HPO_4, 100 mM citric acid, and 100 mM $NaNO_3$ (pH = 7.35)). [b]Similar rate constants of association and dissociation were also observed for duplex **X15** ^{DMA}**T**-T when measurements were conducted in a buffer containing 10 mM cacodylic acid and 100 mM $NaClO_4$ (pH = 6.8). [c]Equilibrium dissociation constants (K_d) were calculated as $K_d = k_{off}/k_{on}$.

DOI: 10.1021/jacs.6b09044
J. Am. Chem. Soc. 2016, 138, 14733–14739

k_{off} was calculated from the obtained half-lives ($t_{1/2}$) (eqs 11 and 12, SI). Similar k_{off} values were obtained for all three duplexes evaluated, ranging from 1.5−9.0 × 10^{-4} s^{-1} (Table 2), corresponding to $t_{1/2}$ values of 0.3−1.3 h.

T-Hg^{II}-T Base Pairs Inhibit DNA−DNA Strand Displacement. Most biochemical processes take place on time scales ranging from microseconds to seconds. The exceptionally high kinetic stabilities of T-Hg^{II}-T base pairs could therefore pose significant barriers to DNA metabolism. To evaluate this possibility, DNA−DNA strand displacement was selected as a model system for T-loop and R-loop dynamics.[29] Duplexes with a short single-stranded overhang (green, Figure 5 and

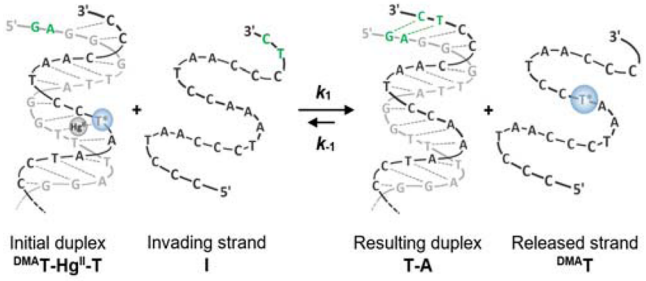

Figure 5. Schematic representation of a strand displacement reaction, where T* = ^{DMA}**T**.

Table S2, SI) were prepared containing either ^{DMA}**T**-Hg^{II}-T or a ^{DMA}**T**-A base pair located three base pairs away from an unmodified T-Hg^{II}-T. Strand displacement of the ^{DMA}**T**-containing strand was initiated by adding a large excess of an unlabeled invading strand "I" to give a longer, thermodynamically more stable duplex as the product. Changes in ^{DMA}**T** fluorescence were used to track strand displacement reactions in real time (Figures S11−S16, SI). Second-order rate constants were calculated under pseudo-first order conditions (eq 14, SI) by adding 4, 6, 8, or 10 equiv of the invading strand. In the absence of Hg^{II}, the rate constants for all duplexes ranged from 29 to 247 M^{-1} s^{-1}, corresponding to experimental half-lives of 1.5−33 min. In contrast, 100- to 2000-fold lower rate constants (k = 0.05−0.47 M^{-1} s^{-1}) were measured for the same duplexes containing a single ^{DMA}**T**-Hg^{II}-T or T-Hg^{II}-T, corresponding to experimental half-lives of 10−77 h. Duplexes lacking a T-T mismatch exhibited the same rates of displacement in the presence and absence of Hg^{II} (Table 3), indicating that nonspecific Hg^{II}-DNA binding had little or no impact on

Table 3. Second-Order Rate Constants k (M^{-1} s^{-1}) of Strand Displacement in the Absence or Presence of Hg^{II}[a]

initial duplex	k (M^{-1} s^{-1}), no Hg^{II}	k (M^{-1} s^{-1}), +Hg^{II}
X13 ^{DMA}**T**-T	97 ± 12	0.05 ± 0.01
X13 ^{DMA}**T**-A, **X10** T-T	55 ± 15	0.47 ± 0.03
X13 ^{DMA}**T**-A, **X16** T-T	247 ± 16	0.21 ± 0.06
X13 ^{DMA}**T**-A	29 ± 3.0	22 ± 3.0[b]

[a]Reported values = mean ± standard deviation of three independent rate constant measurements. All samples contained 4 μM of duplex DNA in aqueous buffer (200 mM Na_2HPO_4, 100 mM citric acid, and 100 mM $NaNO_3$ (pH = 7.35)). ^{DMA}**T**-Hg^{II}-T and T-Hg^{II}-T base pairs were generated by incubating the DNA with 2 equiv of $Hg(ClO_4)_2$ for 3 h. Similar results were obtained when the probe was positioned at **X14** (Figure S16, Table S3, SI). [b]This rate constant was estimated from a single "I" concentration; see Figure S13, SI.

strand-displacement kinetics. Taken together, these results demonstrate that T-Hg^{II}-T base pairs impose a large and specific kinetic barrier to passive DNA−DNA strand-displacement reactions.

T-Hg^{II}-T Base Pairs Inhibit DNA Polymerases. To evaluate the potential impact of T-Hg^{II}-T base pairs on energy-dependent strand-displacement reactions, we investigated enzymatic DNA synthesis by two DNA polymerases differing only in their exonuclease (*exo*) activities: DNA Pol I from *E. coli* (5′ to 3′ *exo*+), and the derived "Klenow Fragment" (5′ to 3′ *exo*−). Primer extension assays were conducted using DNA duplexes containing either a T-T or T-A base pair at position #1 (ODN1) or position #7 (ODN2) downstream of a nicked site (arrow, Figure 6a). DNA synthesis therefore

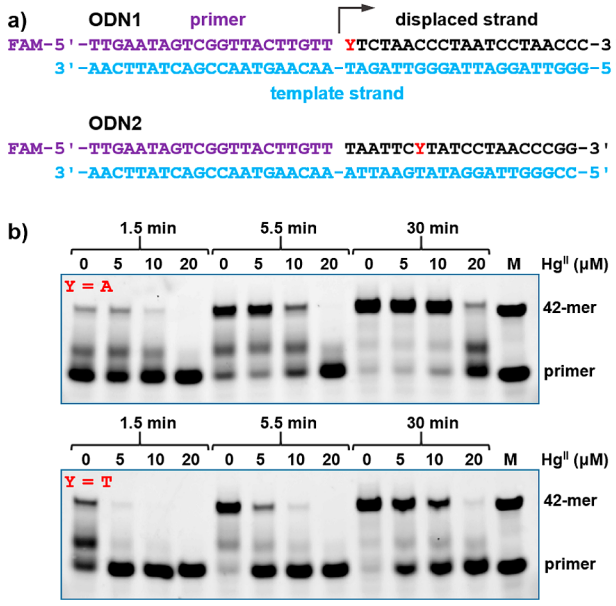

Figure 6. (a) Duplex DNAs "ODN1" and "ODN2" containing a Watson−Crick base pair (Y = A), or T-T mismatch (Y = T) where "FAM" = fluorescein. (b) PAGE analysis of ODN1 primer extension by the Klenow Fragment at various Hg^{II} concentrations and time points. "M" = marker for primer and full-length product.

requires displacement or degradation of the nontemplate "displaced strand" DNA. The primer-template constructs were incubated with variable concentrations of Hg^{II} (0−20 μM) for 3 h, followed by addition of nucleotide triphosphates and a DNA polymerase. Aliquotes from each reaction were removed as a function of time, quenched with EDTA and analyzed by denaturing polyacrylamide gel electrophoresis (PAGE, Figures 6b and S17−S24).

Hg^{II} caused both specific and nonspecific inhibition of primer extension as revealed by duplexes containing T-T versus T-A, respectively. DNA synthesis by the Klenow Fragment (*exo*-) requires DNA strand displacement of the nontemplate strand in a 5′ to 3′ direction. As such, a 2.7-fold higher rate of primer extension was observed for ODN1 containing T-T versus T-A in the absence of Hg^{II} (Table 4). Upon adding 5−10 μM of Hg^{II}, a 7 to 13-fold decrease in k_{obs} was observed for ODN1 containing T-T, whereas little or no change was observed for the same duplex containing a T-A base pair (Klenow, Table 4). Given the relatively slow k_{on} rates for Hg^{II} binding to T-T (Figure 4a), the inhibition of Klenow by T-Hg^{II}-T must be the result of a slow off rate of Hg^{II} from the duplex-enzyme

DOI: 10.1021/jacs.6b09044
J. Am. Chem. Soc. 2016, 138, 14733−14739

Table 4. Observed Rates (k_{obs}) of ODN1 Primer Extension by Klenow Fragment (*exo*−) or *E. coli* DNA Pol I (*exo*+)[a]

Hg^{II} (μM)	"Y"	Klenow (*exo*−) k_{obs} (min^{-1})	k_{obs} rel (*exo*−)	Pol I (*exo*+) k_{obs} (min^{-1})	k_{obs} rel (*exo*+)
0	A	0.18 ± 0.05	1.0	0.20 ± 0.02	1.0
	T	0.48 ± 0.12	1.0	0.21 ± 0.04	1.0
5	A	0.23 ± 0.07	1.3	0.23 ± 0.06	1.2
	T	0.07 ± 0.01	0.15	0.16 ± 0.06	0.76
10	A	0.14 ± 0.05	0.8	0.35 ± 0.16	1.8
	T	0.038 ± 0.002	0.08	0.11 ± 0.05	0.52
20	A	0.044 ± 0.005	0.24	0.17 ± 0.10	0.85
	T	0.04 ± 0.02	0.08	0.05 ± 0.01	0.24

[a]For experimental details, see Materials and Methods. The relative rates "k_{obs} rel" = k_{obs} (X μM Hg)/k_{obs} (0 μM Hg), where X = 5, 10, or 20.

complex. Similar inhibitory effects of a smaller magnitude were observed for ODN2 that exhibited a pronounced stalling and termination of DNA synthesis at the T-Hg^{II}-T site (Figure S21, Table S4, SI).

In contrast to the Klenow Fragment, DNA synthesis by *E. coli* DNA Pol I involves the enzymatic degradation of the nontemplate DNA strand in a 5′ to 3′ direction. As such, in the absence of Hg^{II}, the same rates of primer extension were observed for ODN1 containing T-A versus T-T (Table 4). Interestingly, upon adding 5−10 μM of Hg^{II}, a 2-fold decrease in k_{obs} was observed for ODN1 containing T-T, whereas a roughly 2-fold increase in k_{obs} was observed for ODN1 containing T-A (Pol I, Table 4). These results demonstrate that T-Hg^{II}-T sites impose a specific barrier to DNA synthesis that cannot be entirely overcome by exonuclease activity. Interestingly, the Hg^{II} concentrations needed for DNA polymerase inhibition in vitro (IC_{50} = 6.3−17.5 μM, Figures S18 and S22, SI) were in the same concentration range as those reported to perturb DNA synthesis in living cells.[5]

DISCUSSION AND CONCLUSIONS

The formation and properties of "all-natural" metallo base pairs such as T-Hg^{II}-T and C-Ag^{I}-C have broad implications in materials and biological sciences.[30] Previous studies have demonstrated that T-Hg^{II}-T base pairs exhibit similar thermal stabilities and structural features as T-A base pairs in duplex DNA.[10−12] The perception of analogous behavior of T-Hg^{II}-T and T-A was further enhanced by studies showing that T-Hg^{II}-T could serve as a substitute for T-A in primer hybridization,[13] and by the enzymatic misincorporation of dTTP across from thymidine to give T-Hg^{II}-T base pairs in the new duplex.[14] This activity could provide a pathway for the formation of T-Hg^{II}-T base pairs in genomic DNA that explains some of the point mutations known to occur in cells treated with Hg^{II}.[3]

The kinetic parameters of mercury binding reactions are expected to be highly relevant in vivo, where high concentrations of protein thiols and glutathione (20−50 mM total) would be expected to easily outcompete DNA for Hg^{II} binding.[31] Amazingly, the addition of micromolar concentrations of Hg^{II} (5 μM) to living cells resulted in the formation of high-stability DNA-Hg^{II} adducts at a frequency of 0.3% of all base pairs.[7] This is approximately the same concentration of Hg^{II} that was needed to inhibit DNA polymerase activity in vitro (Table 4) and to perturb DNA synthesis in living cells.[5b] Given the vast excess of intracellular thiols and irreversible binding of S-Hg^{II}-S, thermodynamic parameters alone cannot explain these observations.

Here we report the first kinetic analysis of Hg^{II} binding to T-T sites in duplex DNA. Contrary to the common perception of analogous structural and functional properties of T-Hg^{II}-T and T-A,[10−14] our results demonstrate that T-Hg^{II}-T base pairs are kinetically distinct from T-A base pairs. The slow on-rates and extremely slow off-rates of Hg^{II} from T-T are consistent with the formation and breakage of partially-covalent bonds. Agreement between our kinetic and thermodynamic analyses were remarkably good, both giving affinities in the range of K_d = 8−77 nM. In contrast, duplexes lacking a T-T mismatch exhibited local, "nonspecific" Hg^{II} binding affinities of K_d = 0.20−2.0 μM, depending on the coordination strength of the buffer. The nonspecific components of Hg^{II} association reactions were extremely rapid (Figure S7, SI), consistent with outer-sphere binding of divalent ions that are near the diffusion limits.[28] Given these observations together, we propose a model for Hg^{II} exposure of living cells, where long-range electrostatic interactions faciliate rapid, nonspecific association of Hg^{II} with solvent-exposed sites on DNA[9] that offer some temporary protection from cellular thiols. Cells in S-phase then incorporate Hg^{II} ions into DNA as T-Hg^{II}-T mismatches that exhibit high kinetic stabilities and therefore disrupt a wide variety of processes. Here we demonstrate that T-Hg^{II}-T base pairs are inhibitors of DNA polymerases that would normally displace or degrade the nontemplate DNA strand during DNA synthesis. These activities are required for DNA repair and the completion of DNA lagging-strand synthesis.[32] Indeed, Hg^{II} is known to cause the inhibition of both DNA synthesis and repair in living cells.[5,6] The ability of Hg^{II} to inhibit DNA polymerases in vitro also reveals a potential mechanism for its reported ability to cause DNA strand breaks in vivo,[4,5] where molecules that generate DNA−DNA interstrand cross-links can cause DNA strand breaks due to cellular metabolism.[33] The premature termination of DNA synthesis is one such mechanism by which this can occur (Figure S21). It is possible that other dynamic processes such as transcription and DNA repair are also directly inhibited by the high kinetic stabilities of T-Hg^{II}-T base pairs.

MATERIALS AND METHODS

DNA Synthesis. DNA oligonucleotides containing a single ^{DMA}**T** at variable positions "**X**" were synthesized using phosphoramidite chemistry, purified and characterized as previously reported.[26] Oligonucleotide stock solutions were prepared in pure water. Double-stranded oligonucleotides were formed by mixing equal amounts of the complementary oligonucleotides in the indicated buffer and heating to 95 °C for 5 min, and slowly cooling to room temperature over 4 h. ^{DMA}**T**-Hg^{II}-T and T-Hg^{II}-T base pairs were formed by incubating 2 equiv of $Hg(ClO_4)_2$ with duplex DNA for 3 h prior to use.

Thermodynamic Measurements. Equilibrium dissociation constants (K_d) were measured in three independent trials using a Horiba FluoroLog spectrofluorophotometer equipped with a speed stirrer and a temperature controller. Prefolded duplex DNA (4 μM) was diluted to 25 nM in aqueous buffer (200 mM Na_2HPO_4, 100 mM citric acid, 100 mM $NaNO_3$ (pH = 7.35), or alternatively, 10 mM sodium cacodylate-cacodylic acid, 100 mM $Na(ClO_4)_2$ (pH = 6.8) in a 1.5 mL cuvette. Aliquots of $Hg(ClO_4)_2$ were added while stirring at 25 °C and the fluorescent intensity was measured after a 1 h incubation.

Kinetic Measurements. Association rate constants (k_{on}) were measured in three independent trials using a Horiba FluoroLog spectrofluorophotometer equipped with a speed stirrer and a temperature controller. Prefolded duplex DNA (4 μM) in aqueous

DOI: 10.1021/jacs.6b09044
J. Am. Chem. Soc. 2016, 138, 14733−14739

buffer (200 mM Na_2HPO_4, 100 mM citric acid, and 100 mM $NaNO_3$ (pH = 7.35)) was diluted to a final concentration of 0.1 μM in a 1.5 mL cuvette. $Hg(ClO_4)_2$ (2, 4, and 6 equiv) was added while stirring, and the fluorescent intensity was measured as a function of time (λ_{ex} = 370 nm, λ_{em} = 500 nm) at 25 °C.

Dissociation rate constant (k_{off}) measurements were conducted in three independent trials using a Molecular Devices Spectra spectrofluorophotometer with a temperature controller in 384-well plates. Prefolded duplex DNA (4 μM) in aqueous buffer (200 mM Na_2HPO_4, 100 mM citric acid, and 100 mM $NaNO_3$, pH = 7.35) was incubated with 2 equiv of $Hg(ClO_4)_2$ for 3 h at rt. Then, 50 equiv of an unlabeled duplex DNA of the same sequence containing a T-T mismatch was added as a passive Hg^{II} scavenger, and the mixture was rapidly mixed and then overlaid with paraffin oil. The increase of fluorescent intensity was measured as a function of time (λ_{ex} = 370 nm, λ_{em} = 500 nm) at 25 °C. Similar results were obtained when using a scavenger duplex DNA having a different sequence, suggesting the absence of any strand-displacement activity during the k_{off} measurements.

Strand-Displacement Measurements. Strand-displacement reactions were carried out in three independent trials as previously described.[29] To prefolded ^{DMA}**T**-modified duplex DNA (4 μM) containing a 5′-overhang, an excess of invading strand was added (Table S2). The reaction was rapidly mixed, overlaid with paraffin oil, and changes in fluorescent intensity were measured as a function of time (λ_{ex} = 370 nm, λ_{em} = 500 nm) at 25 °C.

Primer Extension Reactions. dNTPs (100 mM solutions), Klenow Fragment (3′ → 5′ *exo*−), and DNA Pol I (*E. coli*) were purchased from New England BioLabs Inc. Prior to use, the buffers were exchanged by ultrafiltration at 12 500*g* utilizing an Amicon Ultra-0.5 centrifugal filter. The buffer solution containing Klenow Fragment (*exo*−) was exchanged with 25 mM Tris-HCl, 1 mM 3,3′,3″-phosphanetriyltris (benzenesulfonic acid) trisodium salt (TPPTS), 0.1 mM EDTA, and 50% glycerol at pH = 7.40. The buffer solution containing DNA Pol I (*E. coli*) was exchanged with 25 mM Tris-HCl, 0.11 mM TPPTS, 11 μM EDTA and 50% glycerol at pH = 7.40.

Template DNA strands were annealed with complementary sequences and a 5′ FAM-labeled primer at 10 μM each. After heating and slow cooling to rt, $Hg(ClO_4)_2$ was added (0−200 equiv) and incubated for 3 h at rt. The mixture was diluted to a final concentration of 100 nM. dNTPs were then added, and the reaction was started by the addition of DNA polymerase. The total reaction volume was 70 μL, and the final concentrations of each component were 100 nM template strand, 100 nM primer, 100 nM complementary strand, 2 μM dNTPs, and 50 nM Klenow Fragment (*exo*−) or 0.05 nM DNA Pol I (*E. coli*). The reaction mixture was incubated at 37 °C (Klenow Fragment) or 25 °C (DNA Pol I). Final buffer conditions were 50 mM NaCl, 10 mM $MgCl_2$ and 10 mM Tris-HCl, 8 μM TPPTS (pH = 7.90). Aliquots of each reaction (10 μL) were removed at the given time point and quenched by the addition of loading solution (10 μL, 8 M urea, 30 mM EDTA, 50% sucrose) and heated at 90 °C for 10 min. The reaction mixtures were then placed on ice and a DTT solution (1 μL, 100 mM) was added to bind Hg^{II} thereby preventing aggregation of the DNA.[14] The reaction components were separated by electrophoresis on a 13% polyacrylamide gel (1× TBE) under denaturing conditions (8 M urea). Gels were scanned on Typhoon FLA 9500 (λ_{ex} = 473 nm, λ_{em} = 520 nm) and analyzed using ImageQuantTL.

■ ASSOCIATED CONTENT

Supporting Information

The Supporting Information is available free of charge on the ACS Publications website at DOI: 10.1021/jacs.6b09044.

Equations, additional figures and tables, and additional fluorescence spectra (PDF)

■ AUTHOR INFORMATION

Corresponding Author

*nathan.luedtke@chem.uzh.ch

Notes

The authors declare no competing financial interest.

■ ACKNOWLEDGMENTS

We gratefully acknowledge the Swiss National Science Foundation for generous financial support (Grant #165949) and the University of Zürich. We thank Franziska Zosel, Prof. Dr. Ben Schuler and his group for their technical assistance.

■ REFERENCES

(1) Park, J.-D.; Zheng, W. *J. Prev. Med. Public Heal.* **2012**, *45*, 344.

(2) Monteiro, D. A.; Rantin, F. T.; Kalinin, A. L. *Ecotoxicology* **2010**, *19*, 105.

(3) (a) Codina, J. C.; Pérez-Torrente, C.; Pérez-Garcia, A.; Cazorla, F. M.; deVicente, A. *Arch. Environ. Contam. Toxicol.* **1995**, *29*, 260. (b) Ariza, M. E.; Williams, M. V. *J. Biochem. Mol. Toxicol.* **1999**, *13*, 107. (c) Schurz, F.; Sabater-Vilar, M.; Fink-Gremmels, J. *Mutagenesis* **2000**, *15*, 525.

(4) Cantoni, O.; Evans, R. M.; Costa, M. *Biochem. Biophys. Res. Commun.* **1982**, *108*, 614.

(5) Williams, M. V.; Winters, T.; Waddell, K. S. *Mol. Pharmacol.* **1987**, *31*, 200.

(6) Christie, N. T.; Cantoni, O.; Sugiyama, M.; Cattabeni, F.; Costa, M. *Mol. Pharmacol.* **1986**, *29*, 173.

(7) Cantoni, O.; Christie, N. T.; Swann, A.; Drath, D. B.; Costa, M. *Mol. Pharmacol.* **1984**, *26*, 360.

(8) (a) Clever, G. H.; Kaul, C.; Carell, T. *Angew. Chem., Int. Ed.* **2007**, *46*, 6226. (b) Megger, D. A.; Megger, N.; Müller, J. In *Metal Ions in Life Sciences*; Sigel, A., Sigel, H., Sigel, R. K. O., Eds.; Springer: Dordrecht, 2012; Vol. *10*, pp 295−317. (c) Takezawa, Y.; Shionoya, M. *Acc. Chem. Res.* **2012**, *45*, 2066. (d) Clever, G. H.; Shionoya, M. In *Metal Ions in Life Sciences*; Sigel, A.; Sigel, H.; Sigel, R. K. O., Eds.; Springer: Dordrecht, 2012; Vol. *10*, pp 269−294.

(9) (a) Katz, S. *Biochim. Biophys. Acta, Spec. Sect. Nucleic Acids Relat. Subj.* **1963**, *68*, 240. (b) Eichhorn, G. L.; Clark, P. *J. Am. Chem. Soc.* **1963**, *85*, 4020. (c) Simpson, R. B. *J. Am. Chem. Soc.* **1964**, *86*, 2059. (d) Buchanan, G. W.; Stothers, J. B. *Can. J. Chem.* **1982**, *60*, 787. (e) Polak, M.; Plavec, J. *Eur. J. Inorg. Chem.* **1999**, *1999*, 547.

(10) Miyake, Y.; Togashi, H.; Tashiro, M.; Yamaguchi, H.; Oda, S.; Kudo, M.; Tanaka, Y.; Kondo, Y.; Sawa, R.; Fujimoto, T.; Machinami, T.; Ono, A. *J. Am. Chem. Soc.* **2006**, *128*, 2172.

(11) Tanaka, Y.; Oda, S.; Yamaguchi, H.; Kondo, Y.; Kojima, C.; Ono, A. *J. Am. Chem. Soc.* **2007**, *129*, 244.

(12) Kondo, J.; Yamada, T.; Hirose, C.; Okamoto, I.; Tanaka, Y.; Ono, A. *Angew. Chem., Int. Ed.* **2014**, *53*, 2385.

(13) Park, K. S.; Jung, C.; Park, H. G. *Angew. Chem., Int. Ed.* **2010**, *49*, 9757.

(14) Urata, H.; Yamaguchi, E.; Funai, T.; Matsumura, Y.; Wada, S.-I. *Angew. Chem., Int. Ed.* **2010**, *49*, 6516.

(15) (a) Liu, J.; Lu, Y. *Angew. Chem., Int. Ed.* **2007**, *46*, 7587. (b) Li, D.; Wieckowska, A.; Willner, I. *Angew. Chem., Int. Ed.* **2008**, *47*, 3927. (c) Liu, C.-W.; Lin, Y.-W.; Huang, C.-C.; Chang, H.-T. *Biosens. Bioelectron.* **2009**, *24*, 2541. (d) Mor-Piperberg, G.; Tel-Vered, R.; Elbaz, J.; Willner, I. *J. Am. Chem. Soc.* **2010**, *132*, 6878. (e) Wang, Z.-G.; Elbaz, J.; Willner, I. *Nano Lett.* **2011**, *11*, 304. (f) Wen, S.; Zeng, T.; Liu, L.; Zhao, K.; Zhao, Y.; Liu, X.; Wu, H.-C. *J. Am. Chem. Soc.* **2011**, *133*, 18312. (g) Thomas, J. M.; Yu, H.-Z.; Sen, D. *J. Am. Chem. Soc.* **2012**, *134*, 13738. (h) Xiao, S. J.; Hu, P. P.; Xiao, G. F.; Wang, Y.; Liu, Y.; Huang, C. Z. *J. Phys. Chem. B* **2012**, *116*, 9565. (i) Kang, I.; Wang, Y.; Reagan, C.; Fu, Y.; Wang, M. X.; Gu, L.-Q. *Sci. Rep.* **2013**, *3*, 2381. (j) Scharf, P.; Müller, J. *ChemPlusChem* **2013**, *78*, 20.

(16) (a) Gruenwedel, D. W.; Cruikshank, M. K.; Smith, G. M. *J. Inorg. Biochem.* **1993**, *52*, 251. (b) Gruenwedel, D. W. *Biophys. Chem.* **1994**, *52*, 115. (c) Tanaka, Y.; Yamaguchi, H.; Oda, S.; Kondo, Y.;

DOI: 10.1021/jacs.6b09044
J. Am. Chem. Soc. 2016, 138, 14733−14739

Nomura, M.; Kojima, C.; Ono, A. *Nucleosides, Nucleotides Nucleic Acids* **2006**, *25*, 613.
(17) (a) Chrisman, R. W.; Mansy, S.; Peresie, H. J.; Ranade, A.; Berg, T. A.; Tobias, R. S. *Bioinorg. Chem.* **1977**, *7*, 245. (b) Uchiyama, T.; Miura, T.; Takeuchi, H.; Dairaku, T.; Komuro, T.; Kawamura, T.; Kondo, Y.; Benda, L.; Sychrovský, V.; Bouř, P.; Okamoto, I.; Ono, A.; Tanaka, Y. *Nucleic Acids Res.* **2012**, *40*, 5766.
(18) (a) Gruenwedel, D. W. *J. Inorg. Biochem.* **1994**, *56*, 201. (b) Kuklenyik, Z.; Marzilli, L. G. *Inorg. Chem.* **1996**, *35*, 5654.
(19) (a) Tanaka, Y.; Ono, A. *Dalton Trans.* **2008**, 4965. (b) Dairaku, T.; Furuita, K.; Sato, H.; Šebera, J.; Yamanaka, D.; Otaki, H.; Kikkawa, S.; Kondo, Y.; Katahira, R.; Bickelhaupt, F. M.; Guerra, C. F.; Ono, A.; Sychrovský, V.; Kojima, C.; Tanaka, Y. *Chem. Commun.* **2015**, *51*, 8488. (c) Jakobsen, U.; Shelke, S. A.; Vogel, S.; Sigurdsson, S. T. *J. Am. Chem. Soc.* **2010**, *132*, 10424.
(20) (a) Torigoe, H.; Ono, A.; Kozasa, T. *Chem. - Eur. J.* **2010**, *16*, 13218. (b) Torigoe, H.; Miyakawa, Y.; Ono, A.; Kozasa, T. *Thermochim. Acta* **2012**, *532*, 28.
(21) (a) Ono, A.; Togashi, H. *Angew. Chem., Int. Ed.* **2004**, *43*, 4300. (b) Liu, C.-W.; Hsieh, Y.-T.; Huang, C.-C.; Lin, Z.-H.; Chang, H.-T. *Chem. Commun.* **2008**, 2242. (c) Wang, J.; Liu, B. *Chem. Commun.* **2008**, 4759. (d) Xue, X.; Wang, F.; Liu, X. *J. Am. Chem. Soc.* **2008**, *130*, 3244. (e) Yang, R.; Jin, J.; Long, L.; Wang, Y.; Wang, H.; Tan, W. *Chem. Commun.* **2009**, 322.
(22) For review articles, see: (a) Okamoto, A.; Saito, Y.; Saito, I. *J. Photochem. Photobiol., C* **2005**, *6*, 108. (b) Sinkeldam, R. W.; Greco, N. J.; Tor, Y. *Chem. Rev.* **2010**, *110*, 2579. (c) Wilhelmsson, L. M. *Q. Rev. Biophys.* **2010**, *43*, 159. (d) Tanpure, A. A.; Pawar, M. G.; Srivatsan, S. G. *Isr. J. Chem.* **2013**, *53*, 366. (e) Jones, A. C.; Neely, R. K. *Q. Rev. Biophys.* **2015**, *48*, 244. (f) Matarazzo, A.; Hudson, R. H. E. *Tetrahedron* **2015**, *71*, 1627.
(23) For selected examples, see: (a) Okamoto, A.; Tainaka, K.; Saito, I. *J. Am. Chem. Soc.* **2003**, *125*, 4972. (b) Sun, K. M.; McLaughlin, C. K.; Lantero, D. R.; Manderville, R. A. *J. Am. Chem. Soc.* **2007**, *129*, 1894. (c) Jiang, D.; Seela, F. *J. Am. Chem. Soc.* **2010**, *132*, 4016. (d) Dumas, A.; Luedtke, N. W. *Nucleic Acids Res.* **2011**, *39*, 6825. (e) Dumas, A.; Luedtke, N. W. *ChemBioChem* **2011**, *12*, 2044. (f) Riedl, J.; Pohl, R.; Rulisek, L.; Hocek, M. *J. Org. Chem.* **2012**, *77*, 1026. (g) Segal, M.; Fischer, B. *Org. Biomol. Chem.* **2012**, *10*, 1571. (h) Saito, Y.; Suzuki, A.; Okada, Y.; Yamasaka, Y.; Nemoto, N.; Saito, I. *Chem. Commun.* **2013**, *49*, 5684. (i) Seio, K.; Kanamori, T.; Tokugawa, M.; Ohzeki, H.; Masaki, Y.; Tsunoda, H.; Ohkubo, A.; Sekine, M. *Bioorg. Med. Chem.* **2013**, *21*, 3197. (j) Weinberger, M.; Berndt, F.; Mahrwald, R.; Ernsting, N. P.; Wagenknecht, H. A. *J. Org. Chem.* **2013**, *78*, 2589. (k) Rodgers, B. J.; Elsharif, N. A.; Vashisht, N.; Mingus, M. M.; Mulvahill, M. A.; Stengel, G.; Kuchta, R. D.; Purse, B. W. *Chem. - Eur. J.* **2014**, *20*, 2010. (l) Suchy, M.; Hudson, R. H. E. *J. Org. Chem.* **2014**, *79*, 3336. (m) McCoy, L. S.; Shin, D.; Tor, Y. *J. Am. Chem. Soc.* **2014**, *136*, 15176. (n) Kanamori, T.; Ohzeki, H.; Masaki, Y.; Ohkubo, A.; Takahashi, M.; Tsuda, K.; Ito, T.; Shirouzu, M.; Kuwasako, K.; Muto, Y.; Sekine, M.; Seio, K. *ChemBioChem* **2015**, *16*, 167. (o) Larsen, A. F.; Dumat, B.; Wranne, M. S.; Lawson, C. P.; Preus, S.; Bood, M.; Gradén, H.; Wilhelmsson, L. M.; Grøtli, M. *Nat. Publ. Gr.* **2015**, 1. (p) Sholokh, M.; Sharma, R.; Shin, D.; Das, R.; Zaporozhets, O. A.; Tor, Y.; Mély, Y. *J. Am. Chem. Soc.* **2015**, *137*, 3185. (q) Mata, G.; Luedtke, N. W. *J. Am. Chem. Soc.* **2015**, *137*, 699. (r) Mizrahi, R. A.; Shin, D.; Sinkeldam, R. W.; Phelps, K. J.; Fin, A.; Tantillo, D. J.; Tor, Y.; Beal, P. A. *Angew. Chem., Int. Ed.* **2015**, *54*, 8713. (s) Tanpure, A. A.; Srivatsan, S. G. *Nucleic Acids Res.* **2015**, *43*, e149.
(24) (a) Fedoriw, A. M.; Liu, H.; Anderson, V. E.; deHaseth, P. L. *Biochemistry* **1998**, *37*, 11971. (b) Arzumanov, A.; Godde, F.; Moreau, S.; Toulme, J.; Weeds, A.; Gait, M. J. *Helv. Chim. Acta* **2000**, *83*, 1424. (c) Bradrick, T. D.; Marino, J. P. *RNA* **2004**, *10*, 1459. (d) Gilbert, S. D.; Stoddard, C. D.; Wise, S. J.; Batey, R. T. *J. Mol. Biol.* **2006**, *359*, 754. (e) Kimura, T.; Kawai, K.; Fujitsuka, M.; Majima, T. *Tetrahedron* **2007**, *63*, 3585. (f) Parsons, J.; Hermann, T. *Tetrahedron* **2007**, *63*, 3548. (g) Lang, K.; Rieder, R.; Micura, R. *Nucleic Acids Res.* **2007**, *35*, 5370. (h) Barbieri, C. M.; Kaul, M.; Pilch, D. S. *Tetrahedron* **2007**, *63*, 3567. (i) Xie, Y.; Dix, A. V.; Tor, Y. *J. Am. Chem. Soc.* **2009**, *131*, 17605. (j) Velmurugu, Y.; Chen, X.; Sevilla, P. S.; Min, J.-H.; Ansari, A. *Proc. Natl. Acad. Sci. U. S. A.* **2016**, *113*, E2296.
(25) (a) Kim, S. J.; Kool, E. T. *J. Am. Chem. Soc.* **2006**, *128*, 6164. (b) Dumas, A.; Luedtke, N. W. *Chem. - Eur. J.* **2012**, *18*, 245. (c) Omumi, A.; McLaughlin, C. K.; Ben-Israel, D.; Manderville, R. A. *J. Phys. Chem. B* **2012**, *116*, 6158. (d) Jana, S. K.; Guo, X.; Mei, H.; Seela, F. *Chem. Commun.* **2015**, *51*, 17301.
(26) Mata, G.; Schmidt, O. P.; Luedtke, N. W. *Chem. Commun.* **2016**, *52*, 4718.
(27) Martell, A. E.; Smith, R. M. *Critical Stability Constants*; Plenum Press: New York, 1979; Vol. *4*, p 394.
(28) (a) Pörschke, D. *Biophys. Chem.* **1976**, *4*, 383. (b) Granot, J.; Feigon, J.; Kearns, D. R. *Biopolymers* **1982**, *21*, 181.
(29) (a) Yurke, B.; Turberfield, A. J.; Mills, A. P.; Simmel, F. C.; Neumann, J. L. *Nature* **2000**, *406*, 605. (b) Turberfield, A. J.; Mitchell, J. C.; Yurke, B.; Mills, A. P.; Blakey, M. I.; Simmel, F. C. *Phys. Rev. Lett.* **2003**, *90*, 118102. (c) Zhang, D. Y.; Winfree, E. *J. Am. Chem. Soc.* **2009**, *131*, 17303. (d) Zhang, D. Y.; Seelig, G. *Nat. Chem.* **2011**, *3*, 103. (e) Genot, A. J.; Zhang, D. Y.; Bath, J.; Turberfield, A. J. *J. Am. Chem. Soc.* **2011**, *133*, 2177. (f) Tang, W.; Wang, H.; Wang, D.; Zhao, Y.; Li, N.; Liu, F. *J. Am. Chem. Soc.* **2013**, *135*, 13628.
(30) Tanaka, Y.; Kondo, J.; Sychrovský, V.; Šebera, J.; Dairaku, T.; Saneyoshi, H.; Urata, H.; Torigoe, H.; Ono, A. *Chem. Commun.* **2015**, *51*, 17343.
(31) Prakash, M.; Shetty, M. S.; Tilak, P.; Anwar, N. *Online J. Health Allied Scs.* **2009**, *8*, 1.
(32) (a) Dianov, G. L.; Prasad, R.; Wilson, S. H.; Bohr, V. A. *J. Biol. Chem.* **1999**, *274*, 13741. (b) Maga, G.; Villani, G.; Tillement, V.; Stucki, M.; Locatelli, G. A.; Frouin, I.; Spadari, S.; Hübscher, U. *Proc. Natl. Acad. Sci. U. S. A.* **2001**, *98*, 14298.
(33) Frankenberg-Schwager, M.; Kirchermeier, D.; Greif, G.; Baer, K.; Becker, M.; Frankenberg, D. *Toxicology* **2005**, *212*, 175.

DOI: 10.1021/jacs.6b09044
J. Am. Chem. Soc. 2016, 138, 14733−14739